

JCTC

Journal of Chemical Theory and Computation

How Different are Electron-Rich and Electron-Deficient π Interactions?

Inacrist Geronimo, Eun Cheol Lee, N. Jiten Singh,* and Kwang S. Kim*

Center for Superfunctional Materials, Department of Chemistry, Pohang University of Science and Technology, Pohang, 790-784, Korea

Received April 5, 2010

Abstract: The intermolecular interaction driven structural change is vital to molecular architecturing. In the Cambridge Structural Database (CSD), we find that the preference for geometrical conformations of electron-deficient π systems is different from those of electron-rich π systems. Indeed, ab initio calculations find that electron-deficient π ring systems should involve different structures and energetics, consistent with the CSD search, due to the electric multipole moments and the decrease in the spatial extent of π -electron density.

Introduction

The rational design of nanomaterials relies on an understanding of noncovalent interactions, including hydrogen bonding and π interactions,¹ which enables the reversible self-assembly of supramolecular aggregates,² folding of proteins,³ and stacking of DNA.⁴ Most studies conventionally employ electron-rich π systems, such as the benzene dimer and mixed complexes with substituted benzene, as a model of aromatic π interactions.⁵ Electron-deficient systems should involve different energetics due to electric multipole moments and a decrease in the spatial extent of π -electron density.^{6–12} Quadrupole moments (Q_{zz} perpendicular to the ring plane) become more positive relative to benzene (Bz) in isoelectronic N-containing heterocycles pyridine (Py), pyrazine (Pz), triazine (Tr), and tetrazine (Tt) (−8.8 DÅ to 3.3 DÅ, Supporting Information). Therefore, it is of importance to investigate the changes of conformational preference against the number of N atoms in the ring ($\#_N$). The structural change is vital to designing intriguing structures for molecular architecture.¹³ Model systems that have been investigated include pyridine,^{7,8} pyrazine,⁹ pyrimidine,^{10,11} and triazine.^{11,12}

* Corresponding author e-mail: kim@postech.ac.kr (K. S. K.), jiten@postech.ac.kr (N. J. S.).

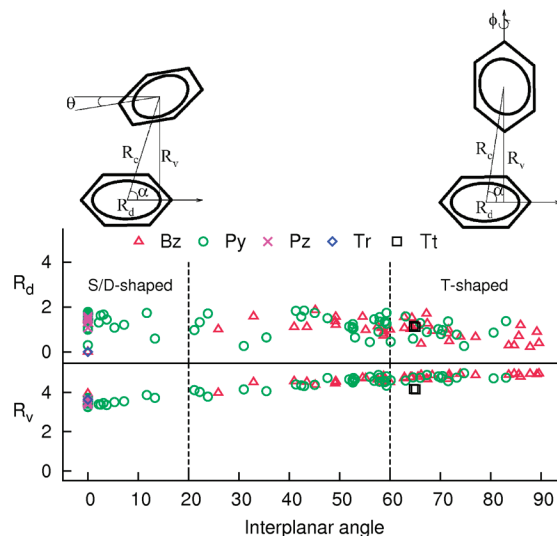


Figure 1. Scatterplots of the horizontal displacement (R_d) and vertical separation (R_v) vs the interplanar angle for benzene (Bz), pyridine (Py), pyrazine (Pz), triazine (Tr), and tetrazine (Tt) for their homopairing in the CSD. Interplanar angles less than 20° are labeled as stacked/displaced-stacked pairs, while those above 60° correspond to T-shaped pairs. The displacement angle is labeled as α . See the Supporting Information (Table S3) for the deviation from coplanarity θ (positive for upward tilt) in the displaced-stacked conformer and the rotation from the xz plane φ (counterclockwise direction taken as positive) in the T-shaped conformer.

Stacking interactions is a recurring motif in crystal structures containing heteroaromatic moieties, as demonstrated by crystal database searches on nitrogen-containing heterocyclic systems.¹⁴ A survey of unsubstituted fragments of N-containing heterocyclic pairs in organic crystals in the CSD indicates a preference for geometrical conformations different from that of benzene (see the Supporting Information for details). Figure 1 is a scatterplot of the horizontal displacement (R_d) and vertical separation (R_v) versus the interplanar angle.

Pairs of Bz moieties generally adopt a T-shaped orientation. Pairs of Py moieties show a wide distribution of displaced-stacked and T-shaped conformers. Pairs of Pz, Tr, and Tt moieties show displaced-stacked, stacked, and nearly T-shaped arrangements, respectively. Antiparallel orientations are observed for stacked and displaced-stacked Py and Tr moieties. T-shaped Py pairs involve C—H $\cdots\pi$ interactions, while Tt pairs have N $\cdots\pi$ (Supporting Information).

Calculations on the pyridine dimer^{7,8} yield a lower binding energy for the antiparallel conformer, and it was further shown by Piacenza and Grimme⁸ using density functional theory with

empirical dispersion corrections that the fully optimized structure is actually slightly bent from the perfect orientation at $\sim 160^\circ$. A cross-displaced stacked dimer was found to be the most stable geometry for pyrazine.⁹ The molecular electrostatic potential of triazine suggests favorable binding for the stacked structure for which the energy had been determined using rigid monomers at a vertical separation of 3.4 Å.¹¹ However, no direct comparison has been made with either fully optimized parallel¹² or antiparallel displaced-stacked conformers. The stacked conformer, for which theoretical studies are rather limited, is generally less stable and was shown to be a maximum in the potential energy curve for the displaced-stacked pyridine dimer.⁷ Detailed symmetry-adapted perturbation theory (SAPT) calculations have been limited to pyridine dimers. Preference for the antiparallel dipole orientation can be traced to electrostatic effects, while induction effects were reported to be an important stabilizing factor in T-shaped conformers. The potential energy curve for the displaced-stacked conformer also shows a decrease in the importance of exchange-repulsion contributions with increasing distance.⁷

Without an understanding of the interactions between electron-deficient π systems, one might still think that it is similar to previously studied π interactions of electron-rich centers. To clarify the issue, we carried out binding energy calculations for diverse electron-deficient π systems comprised of isoelectronic N-containing heterocyclic dimers at the complete basis set (CBS) limit using the coupled cluster theory with single, double, and perturbative triple excitations [CCSD(T)] and analyzed the energy components using SAPT. The systematic and accurate analysis enables us to distinguish the magnitude, directionality, and nature of interaction of electron-deficient π systems from those of well-known electron-rich π systems. To find the trend and origin governing such structural preferences, we investigate the impact of a progressive decrease in the π -electron density of the arene on both geometry and energy. Dimers of Bz ($\#_N = 0$), Py ($\#_N = 1$), Pz ($\#_N = 2$), 1,3,5-Tr ($\#_N = 3$), and 1,2,4,5-Tt ($\#_N = 4$) are used as prototypes.

Computational Method

The resolution of identity approximation of the second-order Møller–Plesset perturbation theory (RI-MP2)¹⁵ using the aug-cc-pVDZ (aVDZ) basis set with basis set superposition error (BSSE) correction was used to optimize the geometries of various parallel and T-shaped structures of pyridine, pyrazine, 1,3,5-triazine, and 1,2,4,5-tetrazine dimers. Single point energy calculations were subsequently performed at the RI-MP2/aug-cc-pVTZ (aVTZ) and CCSD(T)/aVDZ level with BSSE correction to obtain energies at the complete basis set (CBS) limit. The MP2 CBS limit was evaluated by using the extrapolation scheme based on the proportionality of the basis set error in the electron correlation energy to N^{-3} for the aug-cc-pVNZ basis set.¹⁶ This was then used to calculate the CCSD(T)/CBS limit. The total interaction energy was decomposed into electrostatic (E_{es}), induction (E_{in}), dispersion (E_{dp}), and exchange-repulsion (E_{x}) components based on SAPT.¹⁷ Here, E_{in} and E_{dp} includes the exchange-induction term and exchange-dispersion term, respectively, while E_{x} excludes the aforementioned terms from the exchange term. E_{dp} also includes the correction of the dispersion energy based on the difference between the CCSD(T)/

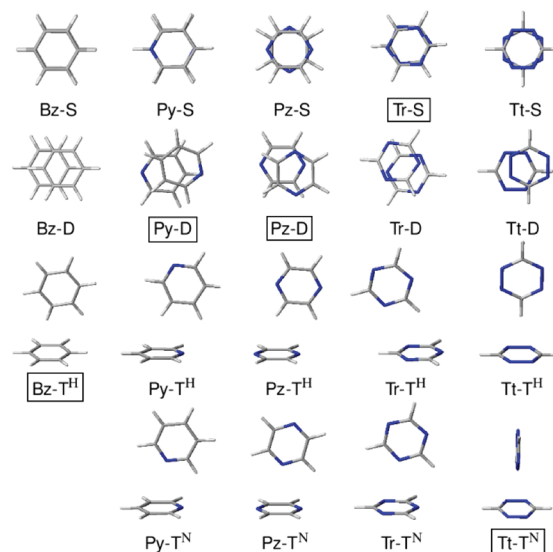


Figure 2. Basis-set-superposition-error (BSSE)-corrected RI-MP2/aug-cc-pVDZ optimized geometries of dimers of Bz, Py, Pz, Tr, and Tt. The lowest energy dimers are enclosed in boxes.

CBS and MP2/aVDZ binding energies (Supporting Information). The CCSD(T)/CBS total energy was added to correct the basis set dependency of the dispersion energy. SAPT calculations were performed with SAPT2008¹⁸ at the MP2/aVDZ' level where the p diffuse functions on H and the d diffuse functions on heavy atoms are removed. RI-MP2 and CCSD(T) calculations were done by using Turbomole 6.0.2¹⁹ and Molpro 2006.1,²⁰ respectively.

Results and Discussion

Stacked (S), displaced-stacked (D), and T-shaped (T^H , $H \cdots \pi$ interaction; T^N , $N \cdots \pi$ interaction) isomers of the Bz, Py, Pz, Tr, and Tt dimers are illustrated in Figure 2. To obtain large electrostatic interactions (either dipole–dipole or quadrupole–quadrupole interactions), the stacked or displaced-stacked Py and Tr dimers show antiparallel orientations between two monomers, while the stacked or displaced-stacked Pz and Tt dimers show perpendicularly rotated orientations. Related binding energies at RI-MP2 and CCSD(T)/CBS, along with the energy components based on SAPT, are summarized in Table 1. Calculations are based on counterpoise-corrected RI-MP2/aVDZ optimized geometries. In order to estimate the errors in the above calculations, we have performed counterpoise-corrected optimization at the RI-MP2/cc-pVTZ and RI-MP2/aug-cc-pVTZ levels. RI-MP2/CBS and CCSD(T)/CBS energies are also estimated by using aVTZ–aVQZ extrapolation (Table 1, Table S4 of the Supporting Information). We find that the results from the counterpoise-corrected optimization at the RI-MP2/cc-pVTZ level for the most stable dimers (Py-D, Pz-D, Tr-S, and Tt- T^N) are closer to those at the RI-MP2/aug-cc-pVDZ optimization. R_c and R_v have an average absolute error of 0.01 Å, while R_d and angle parameters show no significant changes. For the most stable displaced-stacked and T-shaped dimers at the counterpoise-corrected optimization at the RI-MP2/aug-cc-pVTZ level, R_c and R_v have an average absolute error of 0.07 Å, while R_d and angle parameters show no significant changes. RI-MP2/CBS (most stable dimers) and CCSD(T)/CBS energies (Tr-D and Tt-

Table 1. RI-MP2/CBS ($-E_{\text{MP2}}$) and CCSD(T)/CBS ($-E_{\text{tot}}$) Binding Energies Using the aVDZ–aVTZ Extrapolation and SAPT Energy Components (in kcal/mol) of the Selected Low-Energy Dimers (with the Lowest Energy in Bold for Each $\#_N$) at the BSSE-Corrected RI-MP2/aug-cc-pVDZ Geometries^a

| | $-E_{\text{MP2}}$ | $-E_{\text{tot}}$ | $-E_{\text{es}}$ | $-E_{\text{in}}$ | $-E_{\text{dp}}$ | E_{x} |
|-------------------|-------------------|--------------------|------------------|------------------|------------------|----------------|
| Stacked | | | | | | |
| Bz-S | 3.38 | 1.53 | 0.71 | 0.32 | 5.96 | 5.46 |
| Py-S | 4.64 | 2.79 | 2.21 | 0.37 | 6.38 | 6.17 |
| Pz-S | 5.74 | 3.48 | 3.42 | 0.31 | 6.93 | 7.18 |
| Tr-S | 5.00 [5.13] | 3.92 | 2.75 | 0.40 | 6.94 | 6.18 |
| Tt-S | 5.64 | 3.13 | 2.31 | 0.44 | 7.14 | 6.76 |
| Displaced-Stacked | | | | | | |
| Bz-D | 4.93 | 2.62 | 2.92 | 0.96 | 7.89 | 9.14 |
| Py-D | 6.19 [6.20] | 3.80 | 4.48 | 0.99 | 8.11 | 9.78 |
| Pz-D | 6.76 [6.88] | 4.09 | 4.94 | 1.06 | 8.48 | 10.39 |
| Tr-D | 5.22 [5.34] | 3.82 [3.73] | 3.00 | 0.52 | 7.39 | 7.09 |
| Tt-D | 6.47 [6.62] | 3.67 | 3.46 | 1.19 | 8.25 | 9.23 |
| T-Shaped | | | | | | |
| Bz-T ^H | 3.72 | 2.84 | 2.15 | 0.64 | 4.63 | 4.57 |
| Py-T ^H | 4.46 [4.52] | 3.56 ^b | 3.23 | 0.78 | 4.83 | 5.29 |
| Pz-T ^H | 3.50 | 2.70 | 2.20 | 0.65 | 4.42 | 4.56 |
| Tr-T ^H | 2.65 | 2.22 | 1.51 | 0.63 | 3.94 | 3.87 |
| Tt-T ^H | 1.40 | 0.91 | −0.60 | 0.42 | 3.03 | 1.93 |
| Py-T ^N | 3.53 | 2.57 | 2.62 | 1.01 | 4.84 | 5.89 |
| Pz-T ^N | 4.65 [4.72] | 3.36 | 4.76 | 0.93 | 5.23 | 7.57 |
| Tr-T ^N | 4.18 [4.25] | 3.44 | 4.44 | 0.68 | 4.77 | 6.45 |
| Tt-T ^N | 5.70 [5.80] | 4.27 [4.25] | 6.19 | 1.11 | 4.66 | 7.69 |

^a Values in brackets are calculated using the aVTZ–aVQZ extrapolation calculated at the BSSE corrected RI-MP2/aug-cc-pVTZ geometries. ^b Py-T^H is nearly isoenergetic to Py-D.

T^N) derived from the aVDZ–aVTZ extrapolation have average absolute errors of 0.09 and 0.04 kcal/mol, respectively, in comparison with that derived from the aVTZ–aVQZ extrapolation. Thus, there is no significant difference in geometrical parameters and energies with increasing size of basis sets, and hence subsequent discussion will be based on the counterpoise-corrected RI-MP2/aVDZ optimized geometries and CBS energies obtained from the aVDZ–aVTZ extrapolation.

Variation of the binding energy and individual energy components with increasing $\#_N$ is shown in Figure 3. The dominant attractive contribution in the binding energy of benzene with either substituted monomers²¹ or heterocycles⁶ is dispersion, which increases with increasing substitution. The dispersion effects would render electrostatic contributions to the total binding energy (E_{tot}) less significant. The situation is different for the present system and further complicated due to the presence of multipole interactions. For the S series (Bz-S \rightarrow Py-S \rightarrow Pz-S \rightarrow Tr-S \rightarrow Tt-S, solid lines), the binding energy increases only from Bz-S to Tr-S. While the variation in induction binding energy ($-E_{\text{in}} = 0.7 \pm 0.4$ kcal/mol) is small for all cases, the large dispersion binding energy ($-E_{\text{dp}}$) levels off at Pz-S. On the other hand, the electrostatic binding energy ($-E_{\text{es}}$) becomes larger from Bz-S to Pz-S but decreases thereafter. A similar trend is noted for the exchange repulsion energy (E_{x}) except for a particularly small value for Tr-S. Individual energy contributions do not correlate well with E_{tot} except for E_{es} and E_{dp} , which have $R^2 = 0.84$ and 0.76, respectively (E_{in} , $R^2 = 0.17$; E_{x} , $R^2 = 0.48$).

Displaced-stacked structures of the D series (Bz-D \rightarrow Py-D \rightarrow Pz-D \rightarrow Tr-D \rightarrow Tt-D, dashed lines) are more stable than

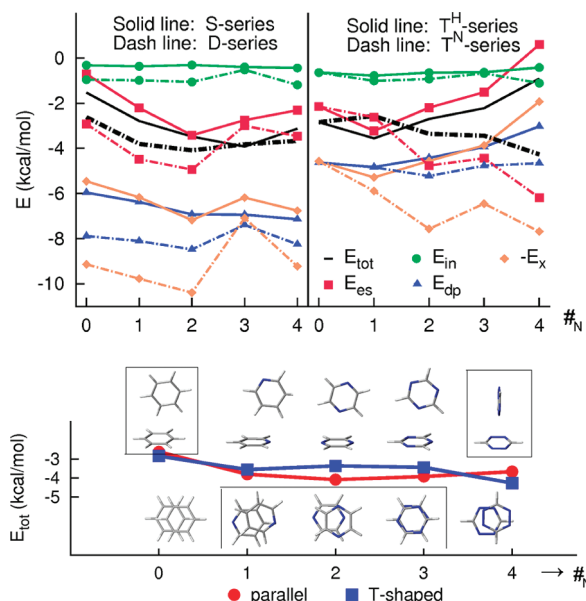


Figure 3. Interaction binding energies and energy components as a function of the number of N atoms ($\#_N$) in a series of dimer complexes. Lowest energy dimers are enclosed in boxes.

the stacked S-series structures, with the exception of Tr-D, which is almost isoenergetic to Tr-S. Stability increases from Bz-D to Pz-D but decreases from Pz-D to Tt-D. As compared with Tz-D, Tr-D has a smaller $-E_{\text{es}}$ and $-E_{\text{dp}}$ but is more stable due to a much smaller E_{x} . Correlation of each energy component with the total binding energy is poor ($R^2 = 0.44, 0.07, 0.01$, and 0.001 for $E_{\text{es}}, E_{\text{dp}}, E_{\text{x}}$, and E_{in} , respectively), reflecting the mixing of $E_{\text{es}}, E_{\text{dp}}$, and E_{x} .

A significant contribution to the stability of the T-shaped isomer of the Bz dimer is C–H $\cdots\pi$ interaction. Nitrogen enhances electrostatic interaction by withdrawing electron density from the ortho or para H, thus increasing its partial positive charge.⁷ However, this is countered by the resulting distortion in the π -electron cloud of the ring, which consequently weakens the C–H $\cdots\pi$ interaction. This trend was observed following the T^H series (Bz-T^H \rightarrow Py-T^H \rightarrow Pz-T^H \rightarrow Tr-T^H \rightarrow Tt-T^H; solid lines in Figure 3), with Tt-T^H having a repulsive electrostatic term. Electrostatic effects become more favorable along the T^N-series (Py-T^N \rightarrow Pz-T^N \rightarrow Tr-T^N \rightarrow Tt-T^N, dash lines), where the orientation is characterized by an N atom pointing toward the positively charged or electron-deficient ring center. In the T^N series, the increase in $-E_{\text{es}}$, however, is tempered by E_{x} as the vertical ring distance becomes shorter. The change in E_{dp} is relatively small from Py to Tt as the distance from the N atom to the ring center is similar. The binding energy for the T^N series correlates well with the electrostatic energy ($R^2 = 0.99$) and poorly with other contributing energy terms. The complexes become more stabilized/destabilized with increasing $\#_N$ for the T^N/T^H series. For the T^H series, all energy components have a good correlation with the total binding energy with $R^2 \rightarrow \sim 0.9$.

Predicted geometries and energetics reasonably explain the N-containing heterocyclic pairs in organic crystals. The small difference in binding energy of the displaced-stacked and T-shaped isomers for Py pairs is demonstrated by nearly equal distributions in the displaced-stacked and T-shaped regions in

Figure 1. Displaced-stacked Py and stacked Tr pairs have antiparallel dipoles and staggered quadrupole orientations. A Tt pair shows a T-shaped structure. Stable displaced-stacked Pz pairs are observed in the gas phase⁹ (Supporting Information).

Conclusion

In summary, heterocyclic dimers preferentially form a stacked/displaced-stacked arrangement, except for Tt, since Tt-T^N is more stable than Tt-D. Displaced-stacked isomers are more stable than the stacked ones except for Tr. For T-shaped isomers, the most stable Py-T^H has C-H $\cdots\pi$ interaction but changes to N $\cdots\pi$ interaction in the cases of Pz-T^N, Tr-T^N, and Tt-T^N. Dispersion effects dominate, particularly for stacked/displaced-stacked conformers. But, relative stabilities can be inferred mostly from the electrostatic contribution as envisaged by its better correlation with binding energies of the complexes except for the displaced-stacked conformers which are governed by E_{es} , E_{dp} , and E_{x} in a complicated manner.²¹ The present understanding would be very useful for designing diverse characteristic molecular models for intriguing molecular assembling and engineering.

Acknowledgment. This work was supported by NRF (WCU: R32-2008-000-10180-0; EPB Center: 2009-0063312, BK21, GRL) and KISTI (KSC-2008-K08-0002).

Supporting Information Available: Geometrical parameters and energies of all of the calculated dimer complexes along with CSD search data analysis and complete references. This material is available free of charge via the Internet at <http://pubs.acs.org>.

References

- (1) (a) Hunter, C. A.; Sanders, J. K. M. *J. Am. Chem. Soc.* **1990**, *112*, 5525–5534. (b) Hobza, P.; Selzle, H. L.; Schlag, E. W. *Chem. Rev.* **1994**, *94*, 1767–1785. (c) Kim, K. S.; Tarakeshwar, P.; Lee, J. Y. *Chem. Rev.* **2000**, *100*, 4145–4185. (e) Singh, N. J.; Min, S. K.; Kim, D. Y.; Kim, K. S. *J. Chem. Theory Comput.* **2009**, *5*, 515–529.
- (2) Singh, N. J.; Lee, H. M.; Hwang, I.-C.; Kim, K. S. *Supramol. Chem.* **2007**, *19*, 321–332.
- (3) Burley, S. K.; Petsko, G. A. *Science* **1985**, *229*, 23–28.
- (4) Cerny, J.; Kabelac, M.; Hobza, P. *J. Am. Chem. Soc.* **2008**, *130*, 16055–16059.
- (5) (a) Sinnokrot, M. O.; Valeev, E. F.; Sherrill, C. D. *J. Am. Chem. Soc.* **2002**, *124*, 10887–10888. (b) Tsuzuki, S.; Honda, K.; Mikami, M.; Tanabe, K. *J. Am. Chem. Soc.* **2002**, *124*, 104–112. (c) Lee, E. C.; Hong, B. H.; Lee, J. Y.; Kim, J. C.; Kim, D.; Kim, Y.; Tarakeshwar, P.; Kim, K. S. *J. Am. Chem. Soc.* **2005**, *127*, 4530–4537. (d) Sinnokrot, M. O.; Sherrill, C. D. *J. Phys. Chem.* **2006**, *110*, 10656–10668. (e) Podeszwa, R.; Bukowski, R.; Szalewicz, K. *J. Phys. Chem. A* **2006**, *110*, 10345–10354. (f) Kim, E.; Paliwal, S.; Wilcox, C. S. *J. Am. Chem. Soc.* **1998**, *120*, 11192–11193. (g) Ren, R.; Jin, Y.; Kim, K. S.; Kim, D. H. *J. Biomol. Struct. Dyn.* **1997**, *15*, 401–405. (h) Hobza, P.; Selzle, H. L.; Schlag, E. W. *J. Phys. Chem.* **1996**, *100*, 18790–18794.
- (6) Wang, W.; Hobza, P. *Chem. Phys. Chem.* **2008**, *9*, 1003–1009.
- (7) Hohenstein, E. G.; Sherrill, C. D. *J. Phys. Chem. A* **2009**, *113*, 878–886.
- (8) (a) Piacenza, M.; Grimme, S. *Chem. Phys. Chem.* **2005**, *6*, 1554–1558. (b) Mishra, B. K.; Sathyamurthy, N. *J. Phys. Chem. A* **2005**, *109*, 6–8.
- (9) Busker, M.; Svartsov, Y. N.; Haber, T.; Kleinermanns, K. *Chem. Phys. Lett.* **2009**, *467*, 255–259.
- (10) Mignon, P.; Loverix, S.; Geerlings, P. *Chem. Phys. Lett.* **2005**, *401*, 40–46.
- (11) Šponer, J.; Hobza, P. *Chem. Phys. Lett.* **1997**, *267*, 263–270.
- (12) Bates, D. M.; Anderson, J. A.; Oloyede, P.; Tschumper, G. S. *Phys. Chem. Chem. Phys.* **2008**, *10*, 2775–2779.
- (13) (a) Hong, B. H.; Lee, J. Y.; Lee, C.-W.; Kim, K. C.; Bae, S. C.; Kim, K. S. *J. Am. Chem. Soc.* **2001**, *123*, 10748–10749. (b) Lee, J. Y.; Hong, B. H.; Kim, W. Y.; Min, S. K.; Kim, Y.; Jouravlev, M. V.; Bose, R.; Kim, K. S.; Hwang, I.-C.; Kaufman, L. J.; Wong, C. W.; Kim, P.; Kim, K. S. *Nature* **2009**, *460*, 498–501.
- (14) (a) Janiak, C. *J. Chem. Soc., Dalton Trans.* **2000**, 3885–3896. (b) Sony, S. M. M.; Ponnuswamy, M. N. *Cryst. Growth Des.* **2006**, *6*, 736–742.
- (15) Feyereisen, M.; Fitzgerald, G.; Komornicki, A. *Chem. Phys. Lett.* **1993**, *208*, 359–363.
- (16) (a) Helgaker, T.; Klopper, W.; Koch, H.; Noga, J. *J. Chem. Phys.* **1997**, *106*, 9639–9646. (b) Min, S. K.; Lee, E. C.; Lee, H. M.; Kim, D. Y.; Kim, D.; Kim, K. S. *J. Comput. Chem.* **2008**, *29*, 1208–1221.
- (17) Jeziorski, B.; Moszynski, R.; Szalewicz, K. *Chem. Rev.* **1994**, *94*, 1887–1930.
- (18) Bukowski, R. et al. *SAPT2008*; University of Delaware: Newark, DE, 2008. See also ref 17.
- (19) *TURBOMOLE V6.02009*; University of Karlsruhe and Forschungszentrum Karlsruhe GmbH: Karlsruhe, Germany, 2007. Available from <http://www.turbomole.com> (accessed Jun 2010).
- (20) Werner, H.-J. et al. *MOLPRO*, version 2006.1; University College Cardiff Consultants Limited: Cardiff, Wales, U.K., 2006. See <http://www.molpro.net> (accessed Jun 2010).
- (21) (a) Ringer, A. L.; Sherrill, C. D. *J. Am. Chem. Soc.* **2009**, *131*, 4574–4575. (b) Lee, E. C.; Kim, D.; Jurecka, P.; Tarakeshwar, P.; Hobza, P.; Kim, K. S. *J. Phys. Chem. A* **2007**, *111*, 3446–3457. (c) Wheeler, S. E.; Houk, K. N. *J. Am. Chem. Soc.* **2009**, *131*, 4574–4575.

CT100182U